Fabrication of Three Terminal Devices by ElectroSpray Deposition of Graphene Nanoribbons

P. Fantuzzi[1,2,*], L. Martini[1,2], A. Candini[2], V. Corradini[2], U. del Pennino[1,2], Y. Hu[3], X. Feng[4], K. Müllen[3], A. Narita[3], M. Affronte[1,2].

[1] Dipartimento di Scienze Fisiche, Informatiche e Matematiche, Università di Modena e Reggio Emilia, Via G. Campi 213/a – 41125 Modena – Italy

[2] Centro S3 - Istituto di Nanoscienze - CNR, Via G. Campi 213/a - 41125 Modena – Italy

[3] Max Planck Institute for Polymer Research, Ackermannweg 10, D-55128 Mainz, Germany

[4] Center for Advancing Electronics Dresden (CFAED) & Department of Chemistry and Food Chemistry, Technische Universität Dresden, 01062 Dresden, Germany

Abstract

Electrospray deposition (ESD) in ambient conditions has been used to deposit graphene nanoribbons (GNRs) dispersed in liquid phase onto different types substrates, including ones suitable for electrical transport. The deposition process was controlled and optimized by using Raman spectroscopy, Atomic Force Microscopy and Scanning Electron Microscopy. When deposited on graphitic electrodes, GNRs were used as semi-conducting channel in three terminal devices showing gate tunability of the electrical current. These results suggest that ESD technique can be used as an effective tool to deposit chemically synthesized GNRs onto substrates of interest for technological applications.

* Corresponding author at: Dipartimento di Scienze Fisiche, Informatiche e Matematiche, Università di Modena e Reggio Emilia, Via G. Campi 213/a, 41125 Modena, Italy.
E-mail address: paolo.fantuzzi@unimore.it (P. Fantuzzi)

1.Introduction

The use of graphene in electronics is attracting much interest for its potential as constituent material of several devices like transistors, sensors, touchscreens and energy storage devices [1]. Its excellent charge mobility and transparency to the visible light are well established and ready to be exploited, but the use of graphene in electronic devices, such as a field effect transistor (FET), requires the presence of an energy gap in the electronic band structure and viable strategies to achieve this goal are still under exploration. The reduction of the lateral size of the graphene layers down to graphene nanoribbons (GNRs) is an efficient way to induce an energy gap, however as long as the GNRs are obtained by conventional top-down approaches such as lithography [2] or by unzipping of carbon nanotubes [3] , the resulting structure is not controllable, making the electronic properties unpredictable. The use of GNRs with atomically-controlled size is therefore very appealing in this context. Typically, high-quality GNRs are grown in ultra high vacuum on metallic surfaces [4,5], however non-conducting substrate is mandatory for applications in electronics. GNRs with atomically defined edges can be alternatively synthesized in liquid-phase [6,7]; given their huge mass, they cannot be evaporated and the deposition is usually performed by drop casting, possibly functionalizing the surface of insulating substrates [8-10].

Electrospray deposition (ESD) [11-15] is an alternative technique that allows to softly land large and heavy molecules from liquid suspension on to any substrate. ESD has been successfully used for the deposition of giant biomolecules (proteins) [16], fullerenes [17,18], carbon nanotubes [19], molecular nanomagnets [20-23] and nanoparticles [24], thus enabling integration of large molecular units in electronic circuits. Homemade and commercial apparatuses are proposed for ESD in a large variety of designs and sophistications. Briefly, besides the capillary injecting the desired sprayed solution/suspension and the target holding the desired support, an ESD setup may include: 1) stages under differential pressure, leading to an UHV environment where the support (either conducting or insulator) is maintained; 2) one or more stages of electromagnetic lenses that act as mass selectors and/or to (de-)accelerate molecules.

Here we report a feasibility study for the fabrication of three terminal electronic devices made of chemically synthesized GNRs dispersed in tetrahydrofuran (THF) and

deposited by an elementary ESD setup. The idea is to use *jugaad* approach to test the viability of this route. To this end, we control the morphology of the deposited GNR film by optical microscopy, scanning electron microscope (SEM), atomic force microscopy (AFM) and the quantity of deposited material by semi-quantitative Raman spectroscopy. To prove the effectiveness of our approach, GNRs have been deposited on graphitic electrodes and *I-V* characteristics measured at room temperature, showing a pronounced gate tunability of the device current.

2. Experimental Methods

2.1 Electro spray apparatus

The ESD system used in our experiments is the early stage of a *Thermo Finnigan Surveyor* Mass Spectrometer (MSQ). The quadrupole and the mass analyzer stage were not used due to the huge mass of the GNRs having a molecular weight in the order of 10^4–10^5 u. Briefly (see Fig. 1), our Electrospray source is composed by a stainless steel insert capillary, where the solution flows. The capillary is hold at voltage V_c, tunable in a range of ± 5 kV, with respect to the target and the rest of the chamber. It is surrounded by a tube injecting nitrogen and the action of both the gas and the voltage V_c produces an aerosol of liquid droplets. The nitrogen promotes the solvent evaporation from the flying charged droplets: when their charge exceeds the surface tension, fission occurs producing small droplets [25]. The pressure of the nitrogen gas was kept at 4 bar at the entrance of the tube in order to get high flux of clean nitrogen in the whole deposition chamber. The solution is contained in an external syringe and it is driven into the capillary by a pump.

The temperature of the capillary and its casing is tunable up to 650°C. High temperature facilitates the evaporation of the solvent and impedes the blocking of the capillary due to the accumulation of agglomerates. The quantity of solute that is deposited was controlled by the time of surface exposure to the flow and indirectly by the concentration of the solution, while the rate of the syringe pump was kept constant. All the depositions have been carried out in ambient conditions, namely at room temperature and atmospheric pressure.

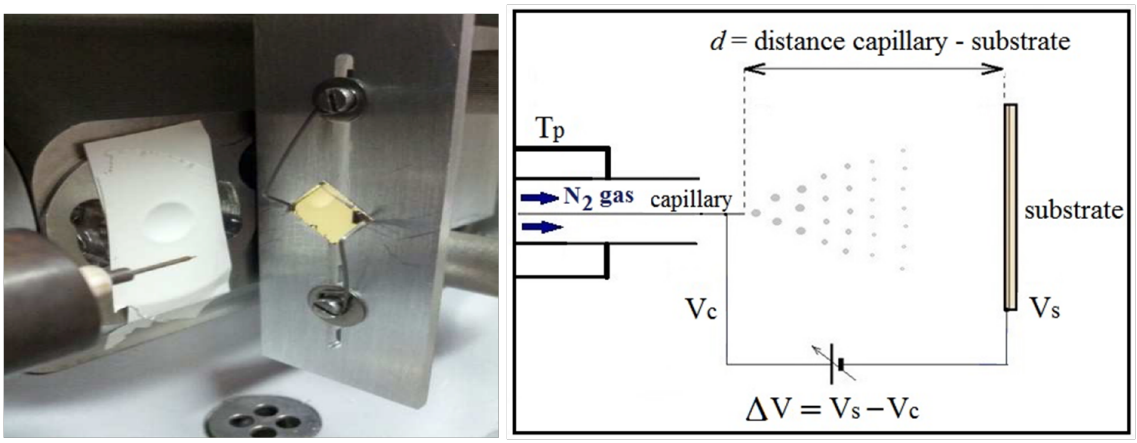

Figure 1: Scheme of the ESD system with the relevant parameters: the probe temperature (T_p), the capillary voltage (V_c) and the sample voltage (V_s) and the distance between substrate and capillary (d).

2.2 Graphene nanoribbons and their dispersion

In this work we used structurally well-defined GNRs with a "cove"-type edge structure and a width of approximately 1 nm (Fig. 2), which were bottom-up synthesized by the methods of synthetic organic chemistry, following a reported procedure [6]. Briefly, the synthesis was carried out through the AB-type Diels-Alder polymerization of a monomeric precursor 2,5-bis-(4-dodecylphenyl)-3-(3-ethynylphenyl)-4-phenyl-2,4-cyclopentadienone to provide non-planar polyphenylene precursors, which were subsequently "graphitized" by oxidative cyclodehydrogenation in solution. Uniform GNRs with the same width and edge structure have thus obtained as powder samples, which could be dispersed in organic solvents such as THF, thanks to the fact that they possess dodecyl ($C_{12}H_{25}$) chains attached at the peripheral positions. Relatively short GNR samples (<100 nm) have been used for the following ESD experiments, considering the decreasing dispersibility of longer GNRs. Two GNR samples with different estimated average lengths, namely approximately 20 and 80 nm, have been examined and gave identical results, at least upon our analysis. Here, the average lengths were roughly estimated based on molecular modeling and weight-average

molecular weights of the corresponding polyphenylene precursors, obtained by the gel permeation chromatography analyses against polystyrene standards.

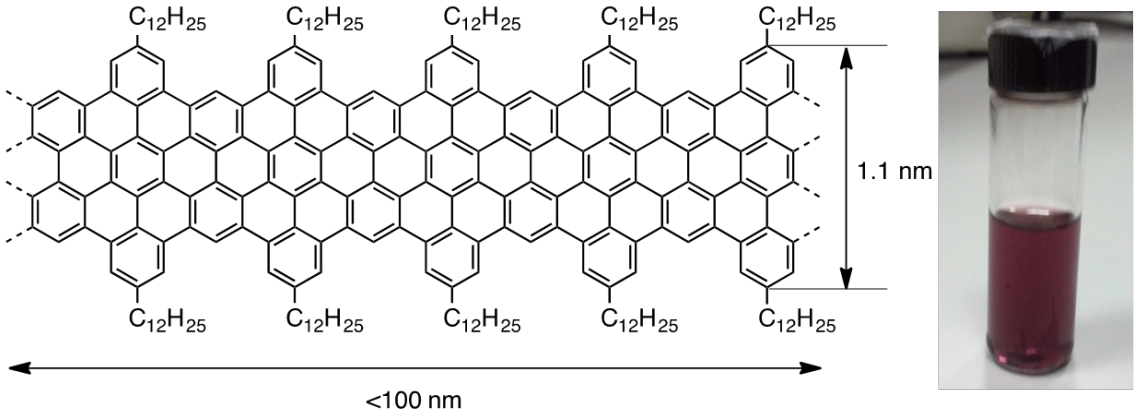

Figure 2: Left: Chemical structure of the GNRs used for the depositions. Right: Mother dispersion S_0 of the GNRs in THF.

In the following, we define "mother dispersion" (S_0) as a supersaturated mixture of GNRs in THF. To obtain good diluted dispersion, S_0 has to be deeply sonicated. To change the concentration, we draw part of S_0 far from the precipitate by a pipette and add THF to make an intermediate dispersion S_1. We refer to S_1=10 (100) to a mixture prepared by diluting S_0 10 (100) times with THF. Since THF is slightly corrosive for the ESD components, the dispersion S_1 is further diluted 10 times with acetonitrile (CH_3CN) to obtain the dispersion S_2 that is actually used for ESD. Since the latter step is performed for all the samples, the concentration of the deposited material is therefore defined only by the dispersion S_1. After the dilution, S_2 was sonicated once more for at least 15 minutes at 40 °C in order to reduce the formation of GNR aggregates. In early tests we have also used methanol instead of acetonitrile, but in this case it was quite difficult to maintain good dispersion and the deposition needed to be done immediately after sonication. The quantity of deposited material can be controlled by changing the concentration of the dispersion S_1 and the time of deposition since the rate of syringe pumping is constant and computer controlled, thus in the following we report the quantity of

deposited material in *ml* of sprayed S_2 dispersion. In our experiments the time of deposition ranged between 10 sec to 40 minutes, suggesting that this approach is a rather fast and efficient way to prepare films of GNRs on different types of substrates.

2.3 Surface techniques

The morphology has been firstly visualized by means of optical microscope (Olympus-BX51M), SEM, AFM and scanning tunneling microscopy (STM), reported in Supplementary Information, at different scales.
We used a Veeco Multi Mode Nano Scope IIIa AFM tuned in tapping mode.
The SEM images were accomplished through the Carl Zeiss Σigma equipped with the GEMINI column (typical acceleration voltage used=2kV) while the STM measurements were carried out by an Omicron UHV VT STM system.
Raman spectra have been collected by using a Jobin Yvom LabRAM with an integrated optical microscope, through which we can select the area to be illuminated. We used a laser's wavelength λ = 632.81 nm and the diameter of the spot was ≈ 1 μm in our typical configuration.

3. Results

3.1 Investigation by optical microscope

We have initially optimized the deposition parameters by systematically changing concentrations and modifying the distance *d* between the capillary and the substrate (see Fig. 1). Quantitative information was obtained by Raman analysis of the characteristic D and G peaks.

Firstly, we used the optical microscope for a preliminary investigation on the deposition.

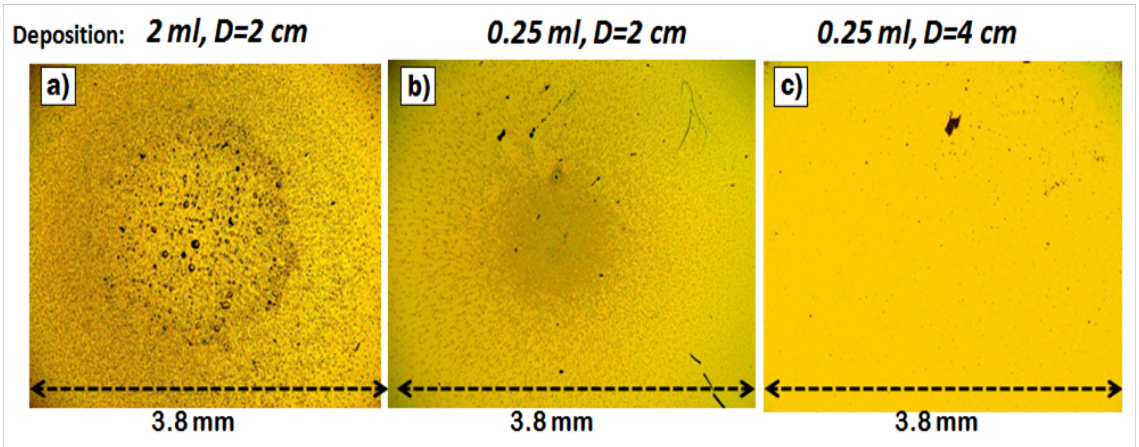

Figure 3: Magnification 5× optical images of Au/mica after ESD of the GNRs with different quantity of dispersion (S_1=10) and different distance d between capillary and substrate:a) 2 ml deposited at d=2 cm. b) 0.25 ml deposited at d=2 cm. c) 0.25 ml deposited at d=4cm.

When the substrate is close to the capillary (*d*=2cm), a central halo is visible in Figure 3a with the clear formation of large aggregates of GNRs. By decreasing the deposited quantity, the homogeneity of the halo increases and the formation of clusters reduces (Fig. 3b). Since the flux injected by the capillary has a conical shape, larger distance *d* between the capillary and the substrate increases the deposition area and the film homogeneity, as a consequence of the reduction of the droplets density. Thus we increased the distance between the substrate and capillaryto *d*= 4cm (Fig. 3c), obtaining a more homogeneous film where the central spot is no longer visible at optical microscope. This test suggests that it is possible to efficiently cover large areas (~cm²) by this technique.

3.2 Investigation by Raman Spectroscopy.

Raman spectroscopy is an efficient tool for studying carbon-based materials [26]. In particular the G peak at ~1600cm^{-1} (which is induced by the in-plane optical phonon branch and therefore is found in all carbon allotropes with sp^2 hybridization) and the D peak at ~1300 cm^{-1} (which is a second order process, in which out-of-plane optical phonons scatter with a defects) are well established in literature to characterize the GNRs [27-30] and a careful analysis of their shape would allow to get information also about the GNR edge [28]. We have simply performed a comparative study of these

peaks to get semi-quantitative information on the quantity of deposited carbon material. A similar approach has been previously employed to study the deposition of carbon nanotubes and the growth of hydrogenated diamond-like carbon films prepared by plasma deposition [31,32]. The background signal due to residual solvent or amorphous material was estimated and subtracted before the measurements of the GNR-deposited samples. In general, the intensity of a Raman peak depends on the laser power, spot size and the penetration depth of the beam. We have therefore took care to perform all the measurement in the same conditions and in a short period of time to avoid the deviation of the laser power. Statistics over the deposited surface was also necessary to account for thickness inhomogeneity (see Supplementary Information for more details).

Fig. 4b and 4c show the trend of the G and D peaks intensity for different deposition conditions on Au/mica. The intensity of both the Raman peaks clearly scales with the quantity of deposited GNR as estimated by the deposition parameters. Similar trends are also obtained considering the area of the respective peaks (see Fig. S2 in Supplementary Information). By decreasing the quantity of deposited GNRs, intensity and areas of both G and D peaks get very small and close to the limit of sensitivity of our measurements that we roughly estimate to be close to 1 monolayer (ML) by comparison with other type of samples.

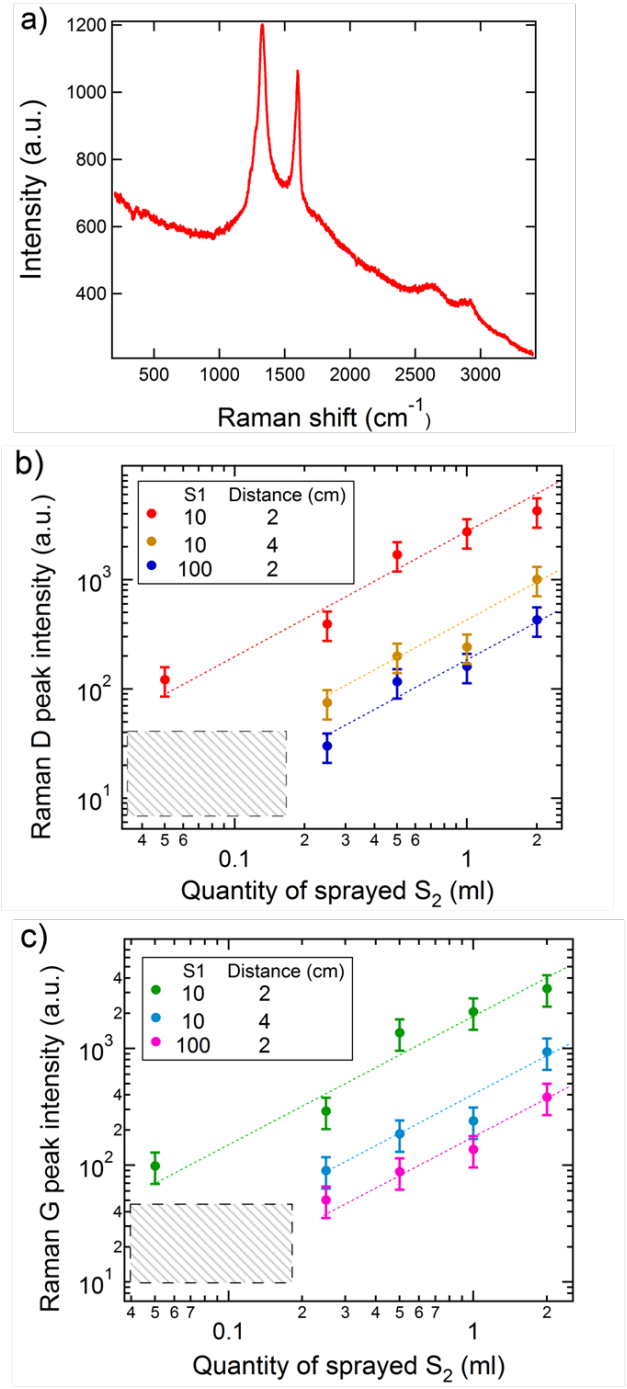

Figure 4:a) Typical Raman spectrum of a GNR film deposited by ESD on Au/mica. b) Intensity of the D peak as a function of the quantity of S_2 deposited for three different deposition conditions. c) Intensity of the G peak.

3.3 Investigation by Scanning Microscopies

To verify the morphology of the surface we used an AFM and a SEM.

Fig. 5 shows AFM images taken in the central region of a GNRs spot deposited on a Au/mica substrate. The deposition parameters were tuned to obtain one of the thinner GNR films according to the semi-quantitative information acquired from Raman (see Fig. 4). In Figure 5a, a network of GNRs bundles is visible at the spot center and we can recognize structures that can be associated to the GNRs with typical dimensions of 2-3 nm in height and 10 to ≈ 100 nm in length (Fig. 5 b, c, d).

Similar results have been obtained by depositing GNRs also on the insulating SiO_2 substrate. Large substrate areas (200μm wide) are homogenously covered by GNRs aggregates: an optical image of 0.25 ml of solution sprayed on a 300 nm thickness of SiO_2 surface over a Si bulk is shown in Fig. 6a. The formation of GNRs aggregates is confirmed by Raman spectra (Fig. 6b) whose intensity at the D and G peaks is very strong on purple spots. On the other hand, in the white shadows the Raman signal is much less intense (Fig. 6c) and it almost disappears (but still detectable) in the blue areas of the optical image. Both the SEM and AFM images better display the morphology of these aggregates, which is probably determined by the slow evaporation of residual solvent.

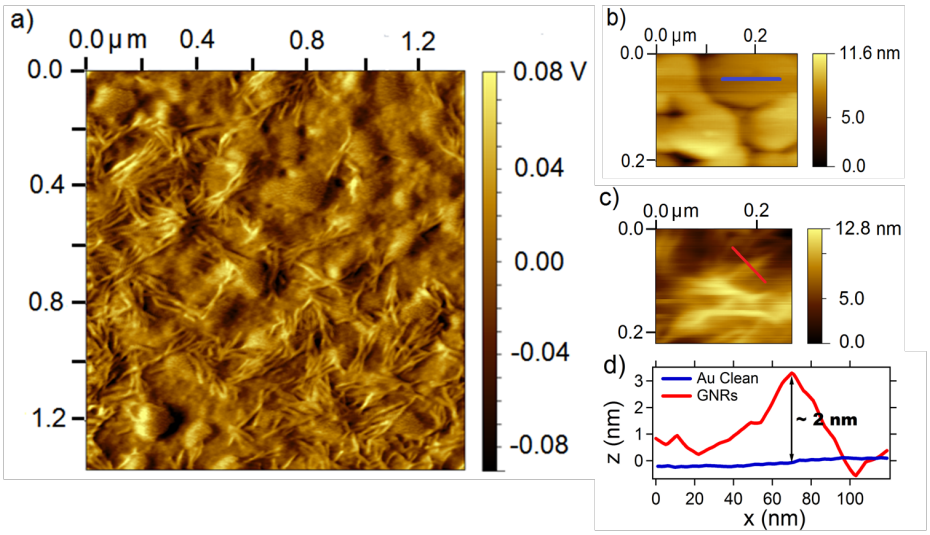

Figure 5: a) Amplitude image of GNRs deposited by ESD of 0.05 ml of S_2(with S_1=10) on Au/mica, distance between capillary and Au/mica = 2 cm. b) AFM image of clean Au/mica substrate. c) ESD of 0.05 ml of S_2 (with S_1=10) on Au/mica. d) Line profiles shown in the images b) and c).

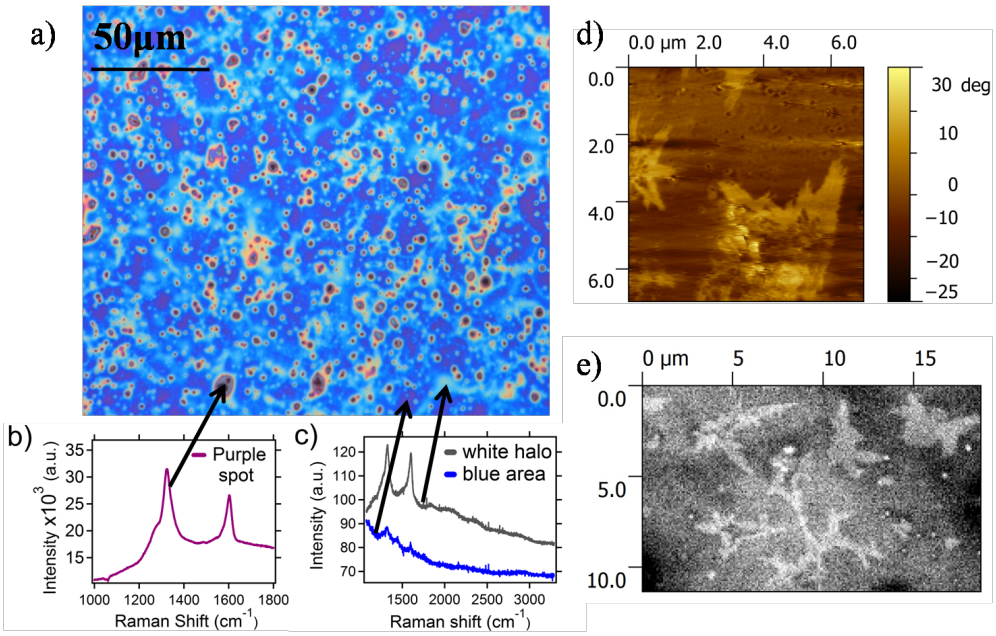

Figure 6: a) Magnification 100× optical image of GNRs deposited by ESD on SiO_2. 0.25 ml of S_1=10, d=4 cm. b) Typical Raman spectrum on the purple spots present on the substrate. c)Typical Raman spectrum on the white regions that surround the purple spots (grey spectrum) and on the blue areas (blue spectrum). d) AFM phase image of the substrate. e) SEM image of the substrate (Magnification =1200×).

3.4 Fabrication and characterization of three terminal device

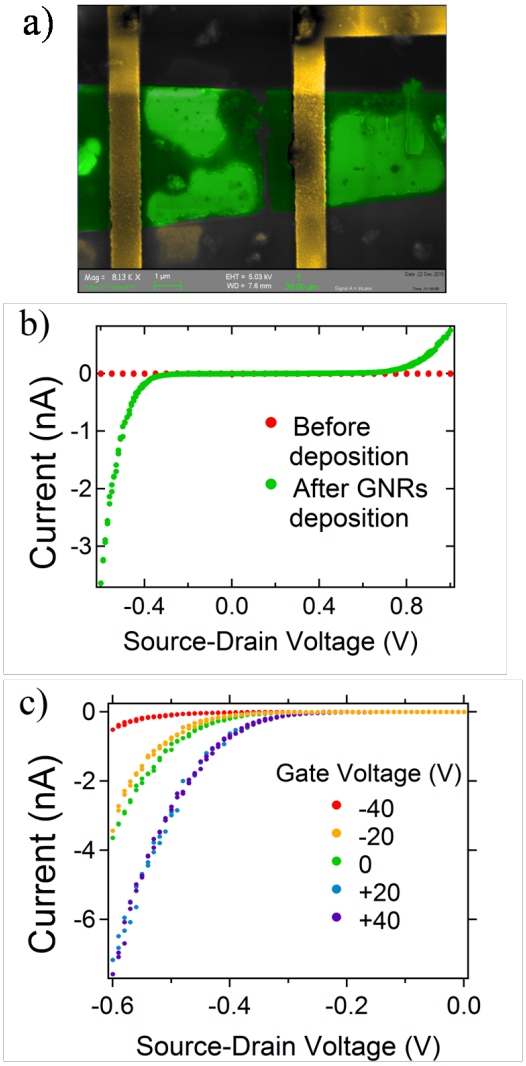

Figure 7:a) SEM image of graphitic contacts made by the electro-burning process [33] on which we deposited 1 ml of S_2 (with S_1=10). The yellow stripes are Cr/Au contacts patterned by EBL, the darker area in the graphene flake (green) is material electro-sprayed on the device: it covers a part of the flake and in particular the gap done by electro-burning. b) I-V characteristics of an electro-burned device before and after the deposition of GNRs through ESD. c) I-V characteristics for different values of the gate voltage.

To test the effectiveness of the ESD method for the realization of GNR-based electronic devices, we have deposited the GNRs on graphitic electrodes on top of a 300-nm-thick SiO_2 substrate, using the underlying doped silicon to make a back gate. The graphitic electrodes were prepared using the electro-burning process [33]. Briefly, multilayer graphene flakes are mechanically exfoliated on the substrate and Cr/Au contacts (typically spaced 1 to 6μm one to another, see Fig.7a) are then fabricated by electron beam lithography (EBL). A physical gap is then opened in the graphitic channel by the electro-burning process [33], setting the parameters to obtain an aperture of the order of~10-50 nm. The opening of the gap can be recognized also by the *I-V* characteristics taken after the electro-burning process, finding no measurable current in the range of –2V to+2V (Fig.7b). After confirming the successful fabrication of the graphitic electrodes (no current passing between source and drain), we deposit GNRs by ESD on the whole substrate and measure again the conductance of the devices. The quantity of sprayed solution (S_2= 1ml) makes reasonable the probability to get GNRs in the region of the gap (Fig. 7a): on a chip with initially ~10electro-burned devices, two of them show a significant increase of conductivity after the GNR deposition (Fig. 7b).

To get reproducible *I-V* characteristics, an annealing at 130°C in vacuum (10^{-7} mbar) is necessary: this likely makes the GNR film more stable on the surface, improving the electrical contact with the graphitic electrodes. After this annealing, the source-drain current I_{SD} is in the nA range for V_{SD} =0.5V. Non linear *I-V* curve probably reflects Schottky barrier at the interface with the electrodes. Interestingly, such *I-V* characteristics show a pronounced gate dependence (Figure 7c), with a current on/off ratio as high as 5. This is higher than what reported for this type of solution-synthesized GNRs [8,9], proving the effectiveness of the ESD as fabrication method. In the previous reports on electrical devices with this type of GNRs the poor gate tunability was generally ascribed to the tendency of the GNRs to form huge aggregates, as the electric field from the back gate is screened by the adjacent ribbons [8,9]. In addition, it has been shown by DFT calculations that the graphene-like band structure (with a vanishingly small energy gap) can be restored as a consequence of the ribbon-ribbon interaction [9]. Here we believe that the electrostatic repulsion between the sprayed GNRs helps to reduce their aggregation, increasing the final response to the applied electric field.

4. Discussion and Conclusions

In this work we have used a simple setup to spray ultra-long solution-synthesized GNRs dispersed in organic solvents. This approach allowed us to circumvent intrinsic and technical difficulties (*e.g.* transfer of GNR on non conducting substrate, evaporation of large mass molecules etc.) that are limiting the use of GNR in electronics. The use of combined analysis allowed us to show that ESD is an efficient way to deposit GNRs on any type of substrates (we tested metallic Au/mica, non conducting SiO_2), and to cover large area as shown by optical microscopy, SEM and AFM on different scales (μm^2 to cm^2). We used semi-quantitative analysis of the G and D Raman peaks to quantify the amount of deposited material and show that it is possible to control the quantity of material deposited through the feeding electrospray source. Three terminal electronic deviceshave been successfully fabricated by electrospray GNRs onto a SiO_2 substrate with graphitic electrodes. *I-V* characteristics show finite current (nA at V_{SD}=0.5V) through the GNR channel and dependence to the gate voltage. Overall, these results show that ESD is a fast deposition technique that represents a valid alternative to drop casting for deposition in ambient conditions.

Further improvements are readily visible adopting suitable technical solutions. For instance, GNRs film homogeneity can be further improved by placing the substrate more distant from the spraying capillary. Additional improvement can potentially be obtained by depositing in a chamber with differential pressure: this may facilitate formation of smaller droplets and improve homogeneity over large surfaces. In commercial mass spectrometer such chamber is placed off axis and after selection of charged molecules and, in the case of GNR, its use results in a drastic reduction of deposition rates. This can be suitable for fabrication of devices comprising single GNR. Alternatively different designs with substrate facing the capillary after chambers with differential pressure may allow efficient deposition also in UHV conditions.

Another interesting parameter of ESD is the application of high potential $\Delta V=V_c-V_s$ between the capillary and the substrates. This has essentially two roles: firstly it ionizes the droplets thus facilitating their dispersion; secondly it charges GNRs. The latter process is necessary to accelerate the GNRs and to select their masses if spectrometer is used. Yet, because of the large mass of GNRs, this process is scarcely

effective and it can be exploited only with a dedicated apparatus. Nevertheless, charged GNRs tend to repulse each other and to better stick on surface. Thus, even if electromagnetic lenses are not used for mass selection, the use of charging potential can help in depositing isolated GNRs on substrate and this can be a further parameter to be controlled.

Acknowledgements.

This work has been partially supported by European Community through the FET-Proactive Project *"MoQuaS",* contract N.610449, and Graphene Flagship (No. CNECT-ICT-604391), by the Italian Ministry for Research (MIUR) through the FIR grant RBFR13YKWX, by the European Research Council grant on NANOGRAPH, and by DFG Priority Program SPP 1459.

References.

[1] http://www.futuremarketsinc.com/graphene-market/

[2] Han MY, Özyilmaz B, Zhang Y, Kim P. Energy Band-Gap Engineering of Graphene Nanoribbons. Phys Rev Lett 2007;98(20):206805. http://dx.doi.org/10.1103/PhysRevLett.98.206805

[3] Kosynkin DV, Higginbotham AL, Sinitskii A, Lomeda JR, Dimiev A, Price BK. Longitudinal unzipping of carbon nanotubes to form graphene nanoribbons. Nature 2009;458(7240):872-6. doi: 10.1038/nature07872

[4] Cai J, Ruffieux P, Jaafar R, Bieri M, Braun T, Blankenburg S, et al. Atomically precise bottom-up fabrication of graphene nanoribbons. Nature 2010;466:470-6. doi:10.1038/nature09211

[5] Baringhaus J, Ruan M, Edler F, Tajeda A, Sicot M, Taleb-Ibrahimi A, et al. Exceptional ballistic transport in epitaxial graphene nanoribbons. Nature 2014;506:349-54. doi:10.1038/nature12952

[6] Narita A, Feng X, Hernandez Y, Jensen SA, Bonn M, Yang H, et al. Synthesis of structurally well-defined and liquid phase-processable graphene nanoribbons. Nat Chem 2014;6:126-32. doi:10.1038/nchem.1819

[7] Narita A, Wang X-Y, Feng X, Müllen K. New advances in nanographene chemistry.Chem Soc Rev 2015;44:6616-43. DOI: 10.1039/C5CS00183H

[8] Abbas AN, Liu G, Narita A, Orosco M, Feng X, Müllen K, et al. Deposition, Characterization, and Thin-Film-Based Chemical Sensing of Ultra-long Chemically Synthesized GrapheneNanoribbons. J Am Chem Soc 2014;136(21):7555–8. DOI: 10.1021/ja502764d

[9] Zschieschang U, Klauk H, Müeller IB, Strudwick AJ, Hintermann T, Schwab MG, et al. Electrical Characteristics of Field-Effect Transistors based on Chemically Synthesized Graphene Nanoribbons. Adv Electron Mater 2015;1(3):1400010. doi: 10.1002/aelm.201400010 (2015)

[10] Konnerth R, Cervetti C, Narita A, Feng X, Müllen K, Hoyer A, et al. Tuning the deposition of molecular graphene nanoribbons by surface functionalization. Nanoscale 2015;7:12807-11. DOI: 10.1039/C4NR07378A

[11] Kitching KJ, Lee H-N, Elam WT, Johnston E, MacGregor H, Miller RJ, et al. Development of an electrospray approach to deposit complex molecules on plasma modified surfaces. Rev Sci Instrum 2003;74(11):4832-9. DOI: 10.1063/1.1618013

[12] Rietveld IB, Kobayashi K, Yamada H, Matsushige K. Electrospray Deposition, Model, and Experiment: Toward General Control of Film Morphology. J Phys Chem B 2006;110(46):23351-64. DOI: 10.1021/jp064147+

[13] Rauschenbach S, Stadler FL, Lunedei E, Malinowski N, Koltsov S, Costantini G, et al. Electrospray ion beam deposition of clusters and biomolecules. Small 2006;2(4):540–7. DOI: 10.1002/smll.200500479

[14] Rauschenbach S, Vogelgesang R, Malinowski N, Gerlach JW, Benyoucef M, Costantini G, et al. Electrospray Ion Beam Deposition: Soft-Landing and Fragmentation of Functional Molecules at Solid Surfaces. ACS Nano 2009;3(10):2901–10. DOI: 10.1021/nn900022p

[15] Hinaut A, Pawlak R, Meyer E, Glatzel T. Electrospray deposition of organic molecules on bulk insulator surfaces. Beilstein J Nanotechnol 2015;6:1927–34. doi:10.3762/bjnano.6.195

[16] Ouyang Z, Takáts Z, Blake TA, Gologan B, Guymon AJ, Wiseman JM, et al. Preparing Protein Microarrays by Soft-Landing of Mass-Selected Ion. Science 2003; 301: 1351. DOI: 10.1126/science.1088776

[17] Satterley CJ, Perdigão LMA, Saywell A, Magnano G, Rienzo A, Mayor LC, et al.Electrospray deposition of fullerenes in ultra-high vacuum: in situ scanning tunneling microscopy and photoemission spectroscopy. Nanotechnology 2007; 18: 455304 doi:10.1088/0957-4484/18/45/455304

[18] Saywell A, Magnano G, Satterley CJ, Perdigão LMA, Champness NR, BetonPHet al. Electrospray Deposition of C_{60} on a Hydrogen-Bonded Supramolecular Network. J Phys Chem C 2008;112(20):7706–9. DOI: 10.1021/jp7119944

[19] O'Shea JN, Taylor JB, Swarbrick JC, Magnano G, Mayor LC, Schulte K. Electrospray deposition of carbon nanotubes in vacuum. Nanotechnology 2007; 18: 035707. doi:10.1088/0957-4484/18/3/035707

[20] Saywell A, Britton AJ, Taleb N, Giménez-López MC, Champness NR, Beton PH, et al. Single molecule magnets on a gold surface: in situ electrospray deposition, x-ray absorption and photoemission. Nanotechnology 2011; 22: 075704. http://dx.doi.org/10.1088/0957-4484/22/7/075704

[21] Corradini V, Cervetti C, Ghirri A, Biagi R, del Pennino U, Timco GA, et al. Oxo-centered carboxylate-bridged trinuclear complexes deposited on Au(111) by a mass-selective electrospray. New J Chem 2011; 35: 1683–1689. DOI: 10.1039/c1nj20080a

[22] Saywell A, Magnano G, Satterley CJ, Perdigão LMA, Britton AJ, Taleb N, et al. Self-assembled aggregates formed by single-molecule magnets on a gold surface. Nat Commun 2010;1:75. doi:10.1038/ncomms1075

[23] Erler P, Schmitt P, Barth N, Irmler A, Bouvron S, Huhn T, et al. Highly Ordered Surface Self-Assembly of Fe_4 Single Molecule Magnets. Nano Lett 2015;15(7):4546−52. DOI: 10.1021/acs.nanolett.5b01120

[24] Bromann K, Félix C, Brune H, Harbich W, Monot R, Buttet J, et al. Controlled Deposition of Size-Selected Silver Nanoclusters. Science 1996;274(5289):956-8. DOI: 10.1126/science.274.5289.956

[25]Jaworek A. Electrospray droplet sources for thin film deposition. J Mater Sci 2007;42:266–97. DOI 10.1007/s10853-006-0842-9

[26] Tuinstra F, Koenig JL, Raman Spectrum of Graphite. J Chem Phys 1970;53:1126. doi: 10.1063/1.1674108

[27] Ferrari AC, Basko DM. Raman spectroscopy as a versatile tool for studying the properties of graphene. Nat Nanotechnol 2013;8:235-46. doi:10.1038/nnano.2013.46

[28] Casiraghi C, Hartschuh A, Qian H, Piscanec S, Georgi C, Fasoli A, et al. Raman Spectroscopy of Graphene Edges. Nano Lett 2009;9(4):1433-41. DOI: 10.1021/nl8032697

[29] Zhou J, Dong J. Vibrational property and Raman spectrum of carbon nanoribbon. Appl Phys Lett 2007;91:173108. doi: 10.1063/1.2800796

[30] Gillen R, Mohr M, Maultzsch J. Raman-active modes in graphenenanoribbons. Physica Status Solidi B 2010;247(11-12):2941-4. DOI10.1002/pssb.201000354

[31] Salzmann CG, Chu BTT, Tobias G, Llewellyn SA, Green MLH. Quantitative assessment of carbon nanotube dispersions by Raman spectroscopy. Carbon 2007;45(5):907-12. doi:10.1016/j.carbon.2007.01.009

[32] Singha A, Ghosh A, Roy A, Ray NR. Quantitative analysis of hydrogenated diamondlike carbon films by visible Raman spectroscopy. J Appl Phys 2006;100:044910. doi: 10.1063/1.2219983

[33] Candini A, Richter N, Convertino D, Coletti C, Balestro F, Wernsdorfer W, et al. Electroburning of few-layer graphene flakes, epitaxial graphene, and turbostratic graphene discs in air and under vacuum. Beilstein J Nanotechnol 2015;6:711–9. doi: 10.3762/bjnano.6.72